

# Numerical evaluation of grading benefits in CdS/CdZnTe band-gap back graded solar cells

YINGHUI SUN\*, PINGXIONG YANG, YE CHEN, LIYAN SHANG, JUNHAO CHU

Key Laboratory of Polar Materials and Devices, Ministry of Education, Department of Electronic Engineering, East China Normal University, Shanghai 200241, People's Republic of China

Recently, incorporation of band-gap graded structure into CdTe absorption layer has been proposed for CdTe based solar cells. In the present work, we numerically investigate the effects of band-gap gradation on photovoltaic characteristics for CdS/CdZnTe band-gap back graded solar cells. Dependences of short circuit current density, open circuit voltage, and conversion efficiency on the grading strength are obtained and analyzed. Moreover, impacts of minority carrier diffusion length of band-gap graded CdZnTe layer on the grading benefits for CdS/CdZnTe back graded solar cells are discussed in detail.

(Received November 12, 2011; accepted February 20, 2012)

**Keywords:** CdS/CdZnTe thin film solar cell, Graded band gap, SCAPS, Photovoltaic characteristics, Minority carrier diffusion length

## 1. Introduction

Cadmium telluride (CdTe) based thin film solar cells are among the best candidates to achieve higher efficiency and lower cost in photovoltaic application [1, 2]. To have better solar cell efficiency, introducing band-gap graded structure into CdTe absorption layer has recently been proposed for CdTe solar cells [3, 4]. In band-gap back graded case, the additional quasi-electric field due to band gap variation has the potential to increase carrier collection probability and to reduce back surface recombination velocity. An analytical model is then developed to estimate the grading benefit on the photocurrent density in band-gap back graded CdZnTe thin films [4].

Numerical solution of carrier transport equations allows a better control of parameters and a more exact estimation of solar cell performances, as comparing to the analytical method. In the present work, we numerically investigate the effects of band-gap gradation on photovoltaic characteristics for CdS/CdZnTe band-gap back grading solar cells by software SCAPS [5]. Variations of short circuit current density, open circuit voltage, and conversion efficiency with the grading strength are calculated and analyzed. Minority diffusion length  $L_n$  is a major transport parameter influencing the carrier collection in the optical absorption layer. Especially in polycrystalline thin films, the values of  $L_n$  vary in a wide range, relying on the grain size and material quality. Therefore, influences of minority carrier diffusion length in band-gap graded CdZnTe layer on the grading benefits for CdS/CdZnTe back graded solar cells will also be discussed.

## 2. Device structure and parameters

The solar cell structure studied here is an  $n\text{-SnO}_2/n\text{-CdS}/p\text{-CdZnTe}$  heterojunction solar cell, with a linearly increased band gap towards the back contact in CdZnTe absorption layer. The band-gap grading strength is defined as the maximum band gap at the rear surface of the cell ( $E_{g\max}$ ). Surface recombination velocities for electrons and holes at the contacts ( $S_n$  and  $S_p$ ) are assumed to be  $10^7$  cm/s. The other parameters with their baseline values for the CdS/CdZnTe solar cells are summarized in Table 1. All the cells in our simulation are operated at the temperature of 300 K. Fig. 1 depicts the energy band diagram for the CdS/CdZnTe back graded solar cell under equilibrium condition with  $E_{g\max} = 1.8$  eV, corresponding the maximum Zn mole fraction  $X_{Zn}$  of 0.2 at the rear surface of the cell. In general,  $p\text{-CdTe}$  and normal metal form deleterious Schottky junction with the barrier height for holes  $\Phi_b = \chi + E_g + \Phi_m$  [8], where  $\Phi_m$  is the work function of the metal. For the case of  $p\text{-Cd}_{1-x}\text{Zn}_x\text{Te}$ , due to the trade-off of decreased electron affinity  $\chi$  and increased band gap  $E_g$  with the Zinc fraction  $x$ , the hole barrier height becomes  $\Phi_b = \Phi_b - 0.04x$ , which is obtained according to the data in Table 1. In our simulation, the front and back contacts are assumed to be ohmic to examine the pure effects of band gap gradation on the solar cell performances.

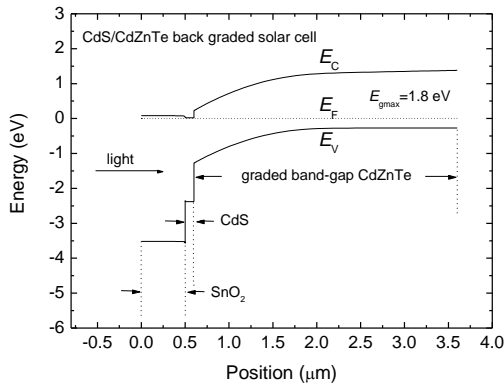


Fig. 1. Energy band diagram of CdS/CdZnTe back graded solar cell under equilibrium condition with the maximum band gap  $E_{gmax}=1.8$  eV at the back contact for CdZnTe.

Table 1. Main parameters with their baseline values in simulating CdS/CdZnTe back graded solar cells at  $T = 300$  K.

Properties	SnO <sub>2</sub> [6]	CdS [6]	Cd <sub>1-x</sub> Zn <sub>x</sub> Te
Thickness ( $\mu\text{m}$ )	0.5	0.1	3
Energy gap $E_g$ (eV)	3.6	2.4	$1.5+0.76x$ [7]
Dielectric constant $\epsilon_r$	9	10	$9.4+0.3x$ [6,7]
Electron affinity, $\chi$ (eV)	4.5	4.5	$4.3-0.8x$ [7]
Electron mobility $\mu_n$ ( $\text{cm}^2/\text{V s}$ )	100	100	320
Hole mobility $\mu_p$ ( $\text{cm}^2/\text{V s}$ )	25	25	40
Effective density of states in conduction band $N_c$ ( $\text{cm}^{-3}$ )	$2.2 \times 10^{18}$	$2.2 \times 10^{18}$	$8 \times 10^{17}$
Effective density of states in valence band $N_v$ ( $\text{cm}^{-3}$ )	$1.8 \times 10^{19}$	$1.8 \times 10^{19}$	$1.8 \times 10^{19}$
Shallow doping density $N_D$ or $N_A$ ( $\text{cm}^{-3}$ )	$N_D, 10^{17}$	$N_D, 10^{18}$	$N_A, 5 \times 10^{14}$

### 3. Results and discussion

In this work, band gap  $E_g$ , electron affinity  $\chi$ , and dielectric constant  $\epsilon_r$  for band-gap graded CdZnTe layer

are position dependent, and other input parameters are assumed to be spatially homogenous, as given in Table 1. The absorption coefficients for CdTe and ZnTe are calculated by using  $\alpha = A(h\nu - E_g)$ , where  $A = 10^5 \text{ cm}^{-1} \text{ eV}^{-1/2}$ . As for Cd<sub>1-x</sub>Zn<sub>x</sub>Te, the absorption coefficients are obtained through interpolation method [9], as depicted in Fig. 2. The default illumination condition is AM1.5 spectrum with the light power of  $100 \text{ mW/cm}^2$ . The carrier generation rate is calculated by using  $G(x) = \alpha\Phi_0 \exp(-\alpha x)$ , where  $\Phi_0$  is the incident photon flux from AM1.5 spectrum.

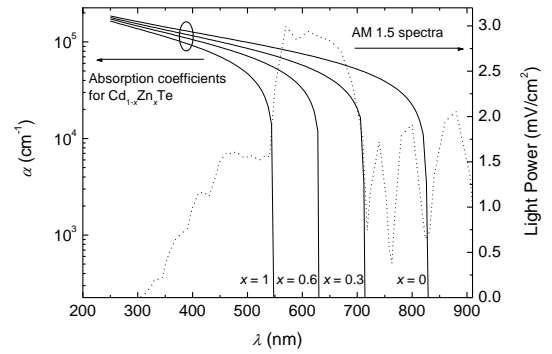


Fig. 2. Absorption coefficients for Cd<sub>1-x</sub>Zn<sub>x</sub>Te with the Zn fraction  $x$  equaling 0, 0.3, 0.6, and 1. The dot curve is AM1.5 spectrum profile.

Fig. 3(a) shows the calculated short circuit current density  $J_{sc}$  as a function of  $E_{gmax}$  for CdS/CdZnTe back graded solar cells with four different values of electron diffusion length  $L_n$  in CdZnTe absorption layer. The monotonic decreases of  $J_{sc}$  with the increment of grading strength are ascribed to the reductions of optical absorption and subsequent carrier generation rate in the cell due to the lifted band-gap grading in CdZnTe absorption layer [10, 11].

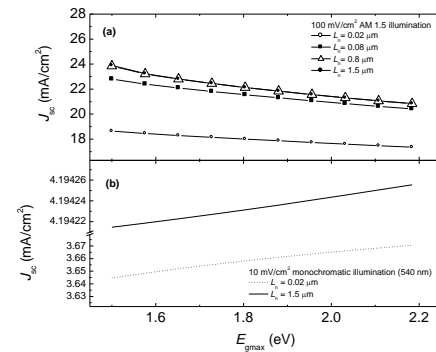


Fig. 3. Dependences of the short circuit current density  $J_{sc}$  on the grading strength defined as  $E_{gmax}$  in CdS/CdZnTe back graded solar cells. Fig. 3(a) is solar cells with  $L_n = 0.02 \mu\text{m}$ ,  $0.08 \mu\text{m}$ ,  $0.8 \mu\text{m}$ , and  $1.5 \mu\text{m}$  under default illumination. Fig. 3(b) is solar cells with  $L_n = 0.02$  and  $1.5 \mu\text{m}$  under 'constant  $G(x)$ ' condition.

To verify the above prediction, we introduce a ‘constant  $G(x)$ ’ condition, in which the loss of  $G(x)$  due to the band-gap gradation is eliminated. We assume  $\Phi_0$  comes from a monochromatic light centered at 540 nm and ranging from 534 nm to 546 nm, with the light power of  $10 \text{ mW/cm}^2$ . The photon energy in this spectrum is lower than band gaps of  $\text{SnO}_2$  and  $\text{CdS}$ , but larger than that of  $\text{CdTe}$ . Meanwhile,  $\alpha$  is set to be a constant of  $10^5 \text{ cm}^{-1}$  for photon energy above  $\text{CdTe}$  band gap. Thus, the carrier generation rate  $G(x)$  keeps the same level when  $\text{CdZnTe}$  graded cells with different values of  $E_{\text{gmax}}$  are illuminated. Through the above strategy, the calculated  $J_{\text{sc}}$  as a function of  $E_{\text{gmax}}$  for two  $\text{CdZnTe}$  graded solar cells is given in Fig. 3(b). The gradually increasing of  $J_{\text{sc}}$  with  $E_{\text{gmax}}$  in Fig. 3(b) is only provided by enhanced carrier collection by the additional quasi-field associated to band-gap gradation, whereas the increment of  $J_{\text{sc}}$  as increased  $E_{\text{gmax}}$  is very weak. Comparing Figs. 3(a) with 3(b), it is seen that the variations of  $J_{\text{sc}}$  with  $E_{\text{gmax}}$  depend on a trade-off between the loss of  $G(x)$  and the gain in carrier collection. In practice, the reduction of  $G(x)$  from band to band absorption exceeds carrier collection increment with increased grading strength if without an effective light trapping, resulting in a lower current output in the solar cell.

As shown in Fig. 3, there is an overall increase of  $J_{\text{sc}}$  for solar cells with larger values of  $L_n$ . The improvement of  $J_{\text{sc}}$  is marginal when  $L_n$  increases from  $0.8 \mu\text{m}$  to  $1.5 \mu\text{m}$ . Moreover, solar cell with lower  $L_n$  shows the slower decrease of  $J_{\text{sc}}$  with  $E_{\text{gmax}}$ , that is, the increased band-gap grading strength has less negative effect on  $J_{\text{sc}}$  for solar cells with smaller  $L_n$ . In Fig. 3(b), the increase of  $J_{\text{sc}}$  with  $E_{\text{gmax}}$  for the cell with  $L_n = 0.02 \mu\text{m}$  is more significant than that in the cell with  $L_n = 1.5 \mu\text{m}$ , indicating band-gap grading tends to give larger improvement in  $J_{\text{sc}}$  to the cell with smaller  $L_n$  for the ‘constant  $G(x)$ ’ case.

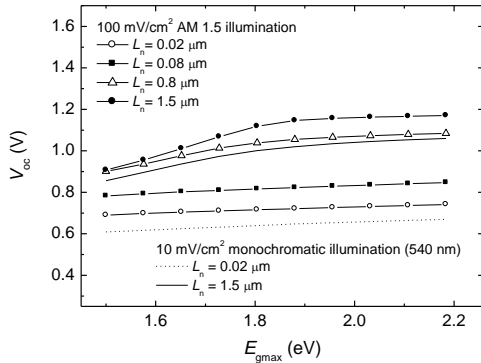


Fig. 4. Dependences of the open circuit voltage  $V_{\text{oc}}$  on the grading strength defined as  $E_{\text{gmax}}$  in  $\text{CdS}/\text{CdZnTe}$  back graded solar cells as described in Fig. 3.

With the increased grading strength, the values of  $V_{\text{oc}}$  increase for all the studied solar cells, as give in Fig. 4. The improvement of  $V_{\text{oc}}$  with increasing  $E_{\text{gmax}}$  is ascribed to the enlarged band gap and reduced carrier recombination in the absorption layer due to band-gap grading. In Fig. 4, solar cells with larger  $L_n$  exhibit higher  $V_{\text{oc}}$  for all the values of  $E_{\text{gmax}}$ . Meanwhile, when  $E_{\text{gmax}}$  increases from  $1.5 \text{ eV}$  to  $1.8 \text{ eV}$ , the improvement of  $V_{\text{oc}}$

for the largest  $L_n$  of  $1.5 \mu\text{m}$  is about  $0.2 \text{ V}$ , as shown by the solid circles in Fig. 4, and for the smallest  $L_n$  of  $0.02 \mu\text{m}$  the rise of  $V_{\text{oc}}$  is only about  $0.02 \text{ eV}$ , as depicted by the open circles in Fig. 4. It can be seen the drift field from band-gap variation exerts positive impacts on  $V_{\text{oc}}$ , particularly for solar cells with larger  $L_n$ .

Dependences of conversion efficiency  $\eta$  on  $E_{\text{gmax}}$  for  $\text{CdS}/\text{CdZnTe}$  back graded solar cells with different values of  $L_n$  are shown in Fig. 5. It can be seen solar cells with larger  $L_n$  have overall higher  $\eta$  for all the possible  $E_{\text{gmax}}$ . As given in Fig. 5(a) for  $L_n = 0.02 \mu\text{m}$ ,  $\eta$  shows a nearly linear increase as a function of  $E_{\text{gmax}}$ , with the maximum rise of about  $0.27\%$  in  $\eta$ . As for the solar cells with  $L_n = 0.08 \mu\text{m}$ ,  $0.8 \mu\text{m}$ , and  $1.5 \mu\text{m}$ , the optimum  $E_{\text{gmax}}$  corresponding to the maximum  $\eta$  is not the largest  $E_{\text{gmax}}$  in simulation, as shown in Figs. (b) to (d). The maximum improvements in  $\eta$  for the just mentioned three solar cells are about  $0.12\%$ ,  $0.5\%$ , and  $1\%$  respectively. The decreases of  $\eta$  when  $E_{\text{gmax}}$  is above the optimum values are ascribed to the loss of optical generation overweighting the carrier collection increment, indicating the improvement of a quasi-drift field on the carrier collection comes to saturation when  $L_n$  is large enough. In the ‘constant  $G(x)$ ’ case,  $\eta$  shows a rise of about  $2.2\%$  under maximum grading profile for solar cell with  $L_n = 0.02 \mu\text{m}$ . As for the solar cell with  $L_n = 1.5 \mu\text{m}$ , the increment of  $\eta$  is around  $5.1\%$  when the largest  $E_{\text{gmax}}$  is applied.

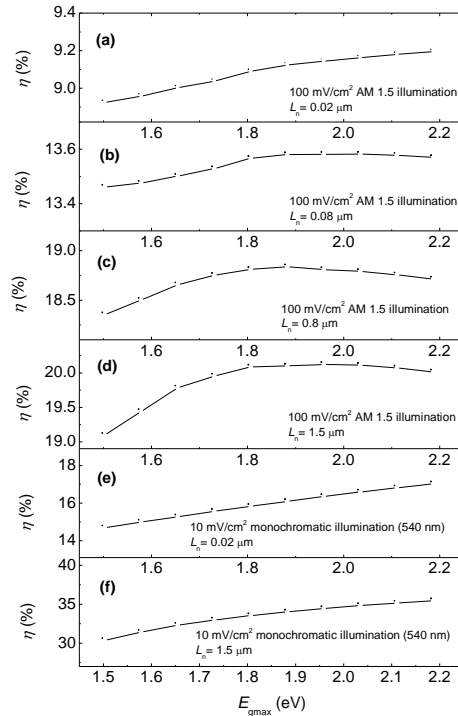


Fig. 5. Dependences of the conversion efficiency  $\eta$  on the grading strength defined as  $E_{\text{gmax}}$  in  $\text{CdS}/\text{CdZnTe}$  back graded solar cells as described in Fig. 3.

From above results, it is predicted that band-gap grading can improve the conversion efficiency of the cell, and solar cells with larger minority diffusion length in the

absorption layer are expected to have higher efficiency for all the values of grading strength. Whereas, the optimum  $E_{gmax}$  is no longer the largest  $E_{gmax}$  that can be used, when  $L_n$  is large enough that carrier collection ability from the quasi-field by band-gap grading is less significant than the loss of optical absorption due to graded band gap.

#### 4. Conclusion

To evaluate the band-gap grading benefits on the performances of CdS/CdZnTe band-gap back graded thin film solar cells, a numerical investigation is carried out by using SCAPS. Photovoltaic characteristics as a function of the grading strength, including short circuit current density, open circuit voltage, and conversion efficiency, are studied. It can be seen that band-gap gradation can improve the open circuit voltage and power conversion efficiency, whereas causes a reduction of short circuit current density due to the loss of optical absorption from band-gap gradation. As expected, solar cells with larger minority carrier diffusion length in the CdZnTe absorption layer have overall better performances. In this work, solar cell with smallest minority diffusion length shows a slower decrease of short circuit current density and a monotonic increase of efficiency with increased grading strength, which is attributed to the effectively enhanced carrier collection ability by the quasi-field from band-gap gradation.

#### Acknowledgements

This work was supported by the National Natural Science Foundation of China (61076060 and 10874127), Science and Technology Commission of Shanghai Municipality (10JC1404600), and Shanghai Postdoctoral Scientific Program (10R21412600).

#### References

- [1] Marc Burgelman, *Thin Film Solar Cells: Fabrication, Characterization, and Applications*, Edited by J. Poortmans and V. Arkhipov, Wiley (2006), pp. 277.
- [2] X. Wu, J. C. Keane, R. G. Dhere, C. DeHart, D. S. Albin, A. Duda, T. A. Gessert, S. Asher, D. H. Levi, P. Sheldon, *Proceedings of the 17th European PVSEC 995* (2001).
- [3] Arturo Morales-Acevedo, *Solar Energy* **83**, 1466 (2009).
- [4] Arturo Morales-Acevedo *Solar Energy Materials and Solar Cells* **95**, 2837 (2011).
- [5] M. Burgelman, P. Nollet, S. Degrave, *Thin Solid Films* **361/362**, 527 (2000).
- [6] M. Gloeckler, J. R. Sites, *J. Appl. Phys.* **95**, 4438 (2004).
- [7] Peter Capper, *Narrow-gap II-VI compounds for optoelectronic and electromagnetic applications*, Springer (1997), pp. 292.
- [8] M. Burgelman, J. Verschraegen, S. Degrave, P. Nollet, *Thin Solid Films* **480–481**, 392 (2005).
- [9] Marc Burgelman and Jonas Marlein, *Proceedings of the 23rd European Photovoltaic Solar Energy Conference, Valencia, Spain* (2008), pp. 2151.
- [10] M. A. Green, *Progress in Photovoltaics: Research and Applications* **17**, 57 (2009).
- [11] M. Troviano, K. Taretto, *Solar Energy Materials and Solar Cells* **95**, 821 (2011).

---

\*Corresponding author: yhsun@mail.sitp.ac.cn